Carcinogenesis, 2017, Vol. 38, No. 7, 738–747

doi:10.1093/carcin/bgx050
Advance Access publication May 23, 2017
Original Manuscript

ORIGINAL MANUSCRIPT

FXR-Gankyrin axis is involved in development of pediatric liver cancer

Leila Valanejad[1], Kyle Lewis[1], Mary Wright[1], Yanjun Jiang[7], Amber D'Souza[3], Rebekah Karns[4], Rachel Sheridan[2], Anita Gupta[2], Kevin Bove[2], David Witte[2], James Geller[3], Gregory Tiao[1], David L.Nelson[6], Lubov Timchenko[5] and Nikolai Timchenko[1,7,*]

[1]Departments of Surgery, [2]Pathology, [3]Oncology, [4]Gastroenterology and [5]Neurology, Cincinnati Children's Hospital Medical Center, 3333 Burnet Ave, Cincinnati, OH, 45229, USA; Baylor College of Medicine, [6]Department of Molecular and Human Genetics, [7]Huffington Center on Aging, One Baylor Plaza, Houston, Texas, 77030, USA

*To whom correspondence should be addressed. Tel: +513-636-0129; Fax: +513-636-1285; E-mail: Nikolai.Timchenko@cchmc.org

Abstract

The development of hepatoblastoma (HBL) is associated with failure of hepatic stem cells (HSC) to differentiate into hepatocytes. Despite intensive investigations, mechanisms of the failure of HSC to differentiate are not known. We found that oncogene Gankyrin (Gank) is involved in the inhibition of differentiation of HSC via triggering degradation of tumor suppressor proteins (TSPs) Rb, p53, C/EBPα and HNF4α. Our data show that the activation of a repressor of Gank, farnesoid X receptor, FXR, after initiation of liver cancer by Diethylnitrosamine (DEN) prevents the development of liver cancer by inhibiting Gank and rescuing tumor suppressor proteins. We next analyzed FXR-Gank-Tumor suppressor pathways in a large cohort of HBL patients which include 6 controls and 53 HBL samples. Systemic analysis of these samples and RNA-Seq approach revealed that the FXR-Gank axis is activated; markers of hepatic stem cells are dramatically elevated and hepatocyte markers are reduced in HBL samples. In the course of these studies, we found that RNA binding protein CUGBP1 is a new tumor suppressor protein which is reduced in all HBL samples. Therefore, we generated CUGBP1 KO mice and examined HBL signatures in the liver of these mice. Micro-array studies revealed that the HBL-specific molecular signature is developed in livers of CUGBP1 KO mice at very early ages. Thus, we conclude that FXR-Gank-TSPs-Stem cells pathway is a key determinant of liver cancer in animal models and in pediatric liver cancer. Our data provide a strong basis for development of FXR-Gank-based therapy for treatment of patients with hepatoblastoma.

Introduction

Liver cancer is the fifth most common cancer and third most common cause of cancer-related death (1,2). The development of hepatocellular carcinoma (HCC) has a long trajectory, affecting mainly adults, while hepatoblastoma (HBL) is a pediatric liver disease, which affects children in the first three years of life. The understanding of molecular mechanisms of HBL and HCC are highly significant for the development of approaches to cure liver cancer. It has been shown that Cancer Stem Cells (CSCs) are elevated in hepatocellular carcinoma (HCC) and might be the source of cancer (1,2). While the elevation of CSCs in liver cancer is well documented, very little is known about the molecular mechanisms of the appearance/elevation of CSCs in the liver. The quiescent state of the liver is supported by several levels of protections. Quiescent livers express up to 20 tumor suppressor proteins (TSPs) (3) and are assumed to be highly protected from the development of HCC and HBL. In addition to well-characterized TSPs, certain micro-RNAs also work as tumor suppressors (4–6). Genome wide methylation analyses revealed that epigenetic control is also involved in support of TSPs (7,8). Among these pathways of levels of protections, numerous

Received: January 23, 2017; **Revised:** April 12, 2017; **Accepted:** May 16, 2017

Abbreviations

CSC	Cancer Stem Cell
DGA	differential gene expression analysis
FXR	farnesoid X receptor
HBL	Hepatoblastoma
HCC	hepatocellular carcinoma
HSC	hepatic stem cell
TSP	tumor suppressor protein

studies provided evidence that TSPs are the key protectors of the liver from the development of cancer (3,9). While there are many tumor suppressors in the liver, Rb, p53, HNF4α C/EBPα and p16, are investigated in great detail as critical inhibitors of hepatocyte proliferation. These proteins might be down-regulated in liver cancer by epigenetic inhibition of transcription, by inhibition of translation, by mutations and by degradation of the proteins.

Despite expression of these TSPs, liver cancer has developed mechanisms by which these TSPs are reduced or neutralized during development of cancer. One of the important mechanisms of neutralizing TSP activities associated with cancer is the activation of a small non-ATP subunit of 26S proteasome, Gankyrin (Gank). Although Gank is a part of the proteasome complex, it shuttles between cellular compartments and triggers degradation of tumor suppressor proteins by different mechanisms. It has been shown that Gank protein is increased in human HCC (10,12). In agreement with these observations, the development of liver cancer in animal models of carcinogenesis also involves activation of Gank (10–13). Particularly, we found that age-associated development of liver cancer is mediated by activation of Gank (14,15). Additionally, Gank eliminates growth inhibitory activities of Rb, p53, HNF4α, and p16. Elimination of C/EBPα, HNF4α, and Rb is mediated by a direct interaction of Gank with these proteins and subsequent degradation (10,12,14). Gank-mediated elimination of p53 is slightly different and it involves activation of MDM2 ligase that triggers degradation of p53 through the UPS system (10). Gank also neutralizes p16 by the replacement of p16 from cdk4 (11). Although Gank is a subunit of proteasome, quiescent livers express low levels of Gank because its promoter is partially repressed by the farnesoid X receptor (FXR) (15). We found that FXR/SHP KO mice spontaneously develop liver cancer at age 12 months and that this development is associated with activation of Gank and subsequent elimination of TSPs (15). The FXR-mediated repression of the Gank promoter is complex and involves activation of complexes repressors C/EBPβ-HDAC1 (15).

Investigations of HBL have intensified during recent years; however, there are very limited studies which address the large scale global alterations of gene expression which occur. There are several publications which examined gene expression in a large cohort of HBL patients. The first study has been performed by Dr. Michalopoulos's group (16). They found a list of genes which presented with higher expression in HBL samples. Among those were fibronectin, DLK1, TGFβ and Mig6 (16). The second global analysis of HBL samples revealed the highly significant role of Wnt-β-catenin signaling in HBL and identified a 16-gene signature associated with aggressive HBL (17). This report and a third report by Cairo et al 2010, provided evidence that HBL has stem cell like signatures (18). The fourth recent paper reports that HBL is a genetically simple tumor with 2.9 mutations per tumor mainly in β-catenin and NFE2L2 genes (19). Therefore, information from these reports suggests that genomic mutations (although important) do not cover the whole range of the complex nature observed in HBL.

In this paper, we performed studies of a large Bio Bank of HBL samples and animal models of liver cancer and we have identified a key pathway of hepatoblastoma. This pathway includes reduction of FXR leading to elevation of Gank and subsequent elimination of tumor suppressor proteins. As the result of these changes, hepatic stem cells fail to differentiate into hepatocytes.

Materials and methods

Antibodies

Antibodies to C/EBPα (14AA), Cyclin D1 (H-295), CUGBP1 (3B1), FXR (H-130), HNF4α (sc-6556), CYP3A4 (HL3), PEPCK (sc-32879), Thy-1 (sc-9163), p53 (sc-6243), cdc2 (sc-53) AFP (sc-8399), PCNA (sc-7907), RB (sc-50), FOXM1 (c-20) and SOCS1 (H-93) were purchased from Santa Cruz Biotechnology (Santa Cruz, CA). Oct4 (Pa1-16943), FOXG1 (Pa5-26794) and EpCam (ab32392), were purchased from ThermoFisher (Fremont, CA). ORM1 (16439-1-AP) and ORM2 (11199-1-AP) were purchased from ProteinTech (Rosemont, IL). Gankyrin (12985S) was purchased from Cell Signal (Danvers, MA). Monoclonal anti-β-actin antibody was purchased from Sigma (St. Louis, MO). Majority of these antibodies were previously used by many investigators including our group. The results are published in previous papers (14,15).

Animal procedures

Male C57BL/6 mice were bred in-house, with free access to food and water on a 12 h dark/light cycle. Mice were injected IP with DEN at 50 μg/g at 3 weeks of age. In experiments with GW4064-mediated activation of FXR, we have used conditions which are described in our previous paper (15). These conditions include pre-treatments of mice with GW4064 for 5 days before DEN injections. These conditions did not affect DEN-mediated initiation of liver cancer, but prevented down-regulation of FXR and up-regulation of Gank which takes place in WT mice within 6 days after DEN injection (15). Livers were harvested at 32–33 weeks post DEN injection and analyzed by histological and biochemical analyses as described below. Generation and overall examination of CUGBP1 knockout mice are described in incoming manuscript (Wei *et al.*, Manuscript Submitted). Since these mice die shortly after birth, they were sacrificed at 3 days of age. RNA was isolated and used for micro-array analysis of gene expression. All mouse studies were approved by the CCHMC Institutional Animal Care and Use Committee (IACUC protocol #IACUC2014-0040).

Normal, background, and HBL pediatric liver samples

Six normal, seven background and fifty-five HBL liver samples were obtained from the Cincinnati Children's Hospital Medical Center Biobank repository in collaboration with the Division of Pathology. Samples we obtained from patients between the ages of 0.01 months to 6 years of age over the course of 10 years. Informed consent was obtained by the patients and families prior to initiation of studies. These protocols were reviewed and approved by the Institutional Review Board at CCHMC (IRB protocol #2015–8826).

Cell culture and chemical treatments

HepG2 cells were purchased from the ATCC (HepG2 [HEPG2] (ATCC®HB-8065). The cells were used immediately after delivery. Cells were authenticated by ATCC before sending. HepG2 cells were treated with DMSO or 10uM OCA for 16 h. RNA and protein extracts were isolated and used for QRT-PCR and Western blotting. Proliferation of HepG2 cells after treatments with OCA was examined using an Invitrogen CyQUANT Cell Proliferation Assay Kit (MP07026). Cells were seeded at 2.5×10^4 and treated with 10 uM OCA for 48 h prior to measuring fluorescence.

Protein isolation and western blotting

Protein extracts were isolated from mouse and human livers and from HepG2 cells as previously described (14,15). Proteins (50 to 100 μg) were loaded on 4–20% gradient gels (Bio-Rad) and transferred to nitrocellulose membranes (Bio-Rad). Membranes were probed with corresponding antibodies. The results of Western blotting analysis are presented by Bar Graphs which show ratios of proteins to loading controls.

Real Time Quantitative Reverse Transcriptase-PCR

Total RNA was isolated from mouse and human livers using RNEasy Plus mini kit (Qiagen) according to the manufacturer's instructions. cDNA was synthesized with 2 µg of total RNA using High-Capacity cDNA Reverse Transcription Kit (ThermoFisher). Gene expression analysis was performed using the TaqMan Universal PCR Master Mix (Applied Biosystems) in a total volume of 10 µl containing 5 µl Master Mix, 1.5 µL water, 3 µl cDNA template and 0.5 µl of the gene-specific TaqMan Assay probe mixture. TaqMan probe mixtures were purchased from Applied Biosystems. The list of these probes can be found in Supplemental Materials.

Liver histology and immunohistochemistry

Liver sections were fixed overnight in 14% PFA, embedded in paraffin and sectioned. 24 hours prior to tissue harvest mice were injected IP with 66.5 mg/kg Bromodeoxyuridine (BrdU) for histological examination. BrdU staining was performed using a BrdU up-take assay kit (Invitrogen).

Micro-array and analysis

Differential gene expression analysis (DGA) was performed between samples derived from three CUGBP1 KO or three wildtype mice. As a result of the DGA, functional group analysis was obtained and annotation enrichment analysis was performed for the candidate genes. Differential expression of genes selected from each category was verified by QRT-PCR as described above. Micro-array results may be accessed in NCBI's GEO with accession number GSE81943.

RNA-Seq analyses of HBL samples

RNA was isolated from 31 HBL patients and from 4 liver samples from healthy patients. RNA sequencing libraries were prepared using Illumina TruSeq RNA preparation kit and sequenced on the Illumina HiSeq 2500, using paired-end, 100 bp reads (Illumina, San Diego, CA). Reads were aligned using hg19 annotations produced by UCSC, and quantified using Kallisto, which accurately quantifies read abundances (in transcripts per million) through pseudoalignment. Statistical analysis was performed in GeneSpring 13.0. Raw counts were thresholded at 1, normalized using quantile normalization procedure, and baselined to the median of all samples (n = 25 240 transcripts). A filtration was applied to ensure analysis of reasonably expressed transcripts, requiring at least two reads in >50% of samples in at least one experimental condition (n = 12 551 transcripts). Ontological analysis of significantly differential genes was performed in the ToppGene Suite. RNA sequencing data may be accessed in NCBI's GEO with accession number GSE81928.

Statistical analysis

All values are presented as means ± SD. Differences between animal groups and background and tumor sections of HBL were determined using a Student t-test. A $^*P < 0.05$ was considered statistically significant.

Results

FXR activation prevents elevation of Gank and reduction of TSPs in DEN protocol of liver cancer

Since FXR KO mice develop spontaneous liver cancer at age of 14 months (20), we asked if the activation of FXR by specific ligands might prevent the development of liver cancer. To test this hypothesis, we have applied the well-characterized DEN-mediated protocol of carcinogenesis. We organized two groups of mice: group 1, 10 male control mice treated with DEN only; group 2, 10 male mice treated with GW4064 (specific activator of FXR) for 5 days and then injected with DEN (Figure 1A, upper). These mice were given GW4064 for 7 additional days. Ten mice of each group were treated with Corn Oil only. Animals were euthanized at 32–33 weeks and the liver masses were examined. We used these time points because this is the earliest time when cancer is detected in WT mice under the DEN protocol. We have previously shown that these conditions for GW4064 treatments specifically blocked down-regulation of FXR within first 7 days after DEN injections and that GW4064 does not interfere with initiation of cancer program (15). To ensure that GW4064 activates FXR in our model for the duration of our study, a separate set of animals were sacrificed at 1 month after DEN injections. We found that GW4064 significantly increases FXR expression in control mice and prevents reduction of FXR in DEN-treated mice 1 month after DEN injections (Figure 1A). Gank is elevated in livers of DEN-treated mice while p53, C/EBPα and HNF4α are reduced (Figure 1B). However, elevation of Gank and reduction of these TSPs are prevented in livers with activated FXR. These results and further examination of FXR pathways in mice 33 weeks after DEN injections (see Figure 2) demonstrated that GW4064 specifically activates FXR and blocks the elevation of Gank and reduction of TSPs in the course of the entire duration of the experiments.

FXR activation prevents liver cancer

Once conditions for the stable FXR-mediated repression of Gank in GW4064/DEN-treated mice were established, we examined tumor nodules in our experimental animals at 33 weeks after DEN injections. We found that all 10 control mice (DEN-treated) develop multiple tumor nodules; while seven mice pre-treated with GW4064 had no nodules (Figure 1C). H&E staining showed that non-tumor liver sections (background) from control DEN mice display a fatty phenotype, but have limited mitotic figures. Tumor sections of control mice show both increased fat droplets and mitotic figures (Figure 1D). Livers of mice with activated FXR contain fewer fat droplets and no mitotic figures. BrdU up-take showed that both non-tumor and tumor sections of control DEN-treated mice have a significant number of replicating hepatocytes; however, activation of FXR inhibits liver proliferation in DEN-treated mice (Figure 1D). Western blotting examination of the FXR-Gank pathway in control, DEN-treated and DEN+GW4064 treated mice at 33 weeks showed that Gank pathway is activated in DEN-treated mice leading to the elimination of TSP (Figure 1E and Supplemental Figure 1). However, activation of FXR by GW4064 rescues the levels of FXR and protects TSPs from degradation. Examination of mRNAs showed no differences (data not shown), suggesting these proteins are degraded in DEN-treated mice, but not in GW4064/DEN-treated mice. Thus, these studies demonstrate that inhibition of Gank through activation of FXR by GW4064 inhibits development of liver cancer under conditions of DEN-mediated carcinogenesis.

Reduction of FXR causes elevation of Gank in HBL samples

With evidence that the FXR-Gank-Tumor Suppressor pathway is a key event in the development of liver cancer in animal models, we hypothesized that this pathway might play a pivotal role in the development of pediatric liver cancer by a block of differentiation of hepatic stem cells (HSC) into mature hepatocytes (Figure 2A). This hypothesis is also based on reports which showed that CSC markers are expressed in HCC and HBL (21). To test the hypothesis, we obtained a large cohort of frozen HBL samples which included 6 control healthy livers from age-matched pediatric patients, 53 HBL (tumor sections) samples and 8 background sections (non-tumor samples of livers with HBL) from the Cincinnati Children's Hospital and Medical Center (CCHMC) Department of Pathology BioBank. All HBL samples were confirmed by pathologists and had significant pathological alterations. H&E staining from a representative patient confirmed aggressive hepatoblastoma with predominantly mildly discohesive undifferentiated cells with high

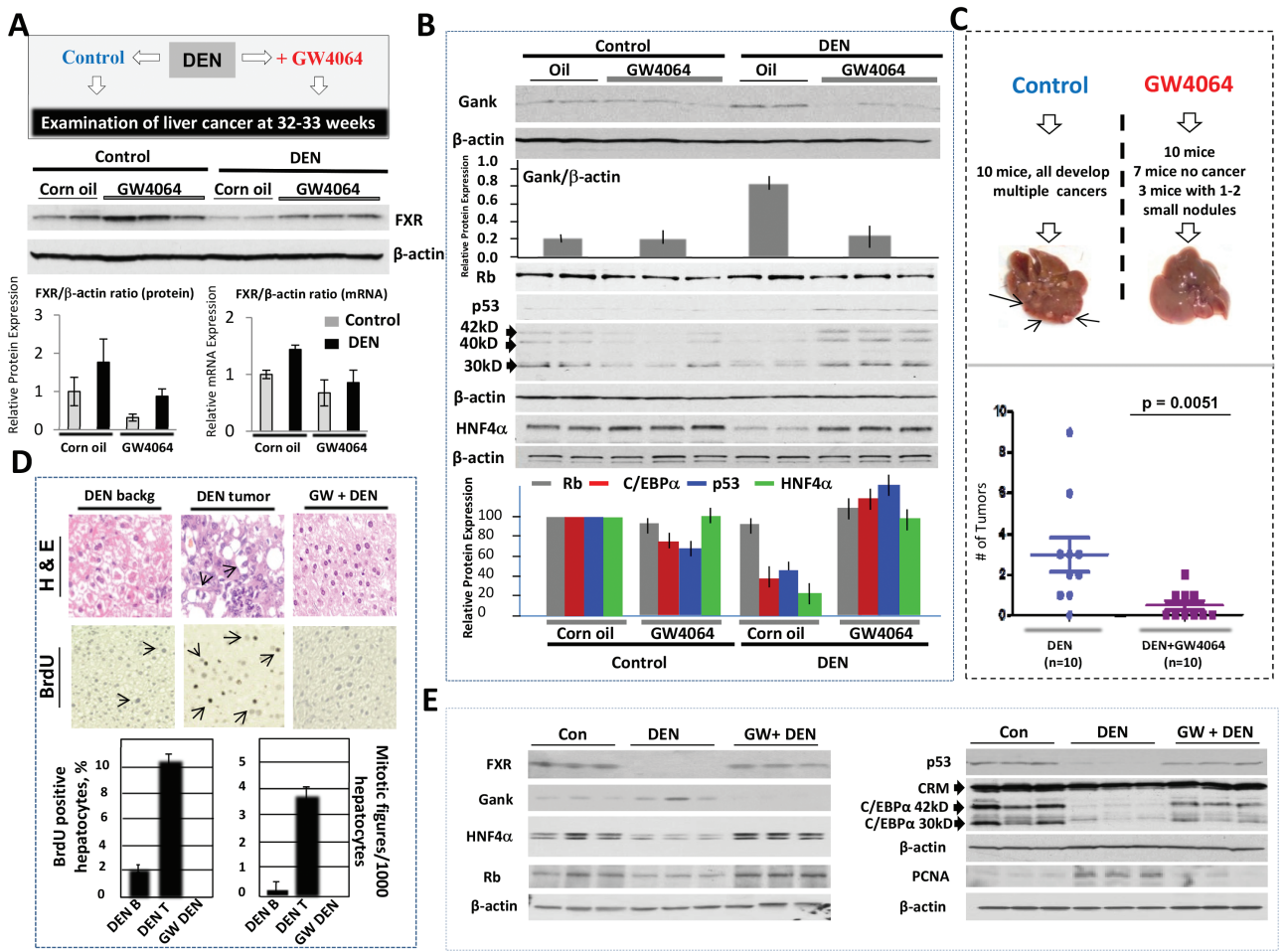

Figure 1. Activation of FXR inhibits liver cancer through blocking elevation of Gankyrin and reduction of tumor suppressor proteins. (**A**) Upper: Design for activation of FXR under DEN-mediated protocol of carcinogenesis. Bottom: Examination of FXR protein and mRNA expression 1 month after initiation of DEN protocol. Western blotting was performed with antibodies to FXR. Membrane was re-probed with Abs to β-actin. Bar graphs show FXR protein expression as a ratio to β-actin as well as changes in mRNA expression normalized to β-actin. (**B**) Examination of protein expression 1 month after initiation of DEN protocol by Western blotting with antibodies shown on the left. 42 kD, 40 kD and 30 kD isoforms of C/EBPα are shown. Membranes were re-probed with Abs to β-actin. Bar graphs show levels of proteins as ratios to β-actin. (**C**) Upper: Tumor nodules in control mice under 33 week DEN protocol compared to tumor nodules in livers of GW4064 treated mice. Bottom: Quantification of tumor nodules in DEN-treated mice as compared to DEN-treated mice under GW4064 treatment. Data represented as mean ± SD; $n = 10$; $P < 0.05$. (**D**) H&E and BrdU staining of liver sections: Arrows show mitotic figures and BrdU-positive hepatocytes. Bar graphs represent % of BrdU positive hepatocytes and number of mitotic figures per 1000 hepatocytes. (**E**) Examination of protein levels by Western blotting in livers of mice 33 weeks after DEN treatments and mice pre-treated with GW4064. Calculations of protein levels as ratios to β-actin are shown in Supplemental Figure 1.

nuclear-to-cytoplasmic ratio, increased mitoses and prominent nucleoli (Figure 2B). Also seen were focal areas of macrotrabecular morphology, with neoplastic cells arranged in plates of >5 cells thick.

The strategy for the investigation of HBL is shown in Figure 2A (right). We also included the investigation of a RNA binding protein, CUGBP1, as a TSP due to recent work in animal models showing that CUGBP1 protects the liver from cancer and Gank eliminates CUGBP1 during development of liver cancer (Lewis *et al.*, under review in MCB). CUGBP1 was initially identified as the protein implicated in myotonic dystrophy (22) and in liver biology (23). Prior to investigations of protein and mRNA expression, all liver samples were examined on the quality of isolated RNA and proteins by gel electrophoresis and by commassie staining. QRT-PCR and Western blotting approaches revealed that FXR mRNA (Figure 2C) and protein (Figure 2D top and bottom) are reduced in a vast majority of samples and that Gank is elevated in all examined HBL samples. Examination of FXR-Gank pathways in additional HBL samples is shown in Supplementary Figure 2. To further examine the causal role of FXR in the down-regulation of Gank in hepatoblastoma cells, we activated FXR in a hepatoblastoma cell line, HepG2, by the synthetic ligand obeticholic acid, OCA. This ligand specifically activates FXR and it is much more potent activator of FXR (24). Western blotting revealed that FXR is elevated in HepG2 cells by OCA and that this elevation resulted in significant repression of Gank on the levels of mRNAs and protein (Figure 2E). This down-regulation is specific since another known target of FXR, small heterodimer partner, SHP, is elevated in OCA treated HepG2 cells (Figure 2E). To determine the functional significance of OCA-dependent stimulation of FXR and reduction of Gank, we examined proliferation of HepG2 cells using two approaches: measurements of proliferation as well as examination of PCNA (S-phase specific) and cdc2 (mitosis-specific) proteins. These studies indicated that activation of FXR and reduction of Gank leads to the inhibition of proliferation (Figure 2F). Taken together, these studies revealed that the reduction of FXR in livers of HBL patients causes activation of Gank and that activation of FXR

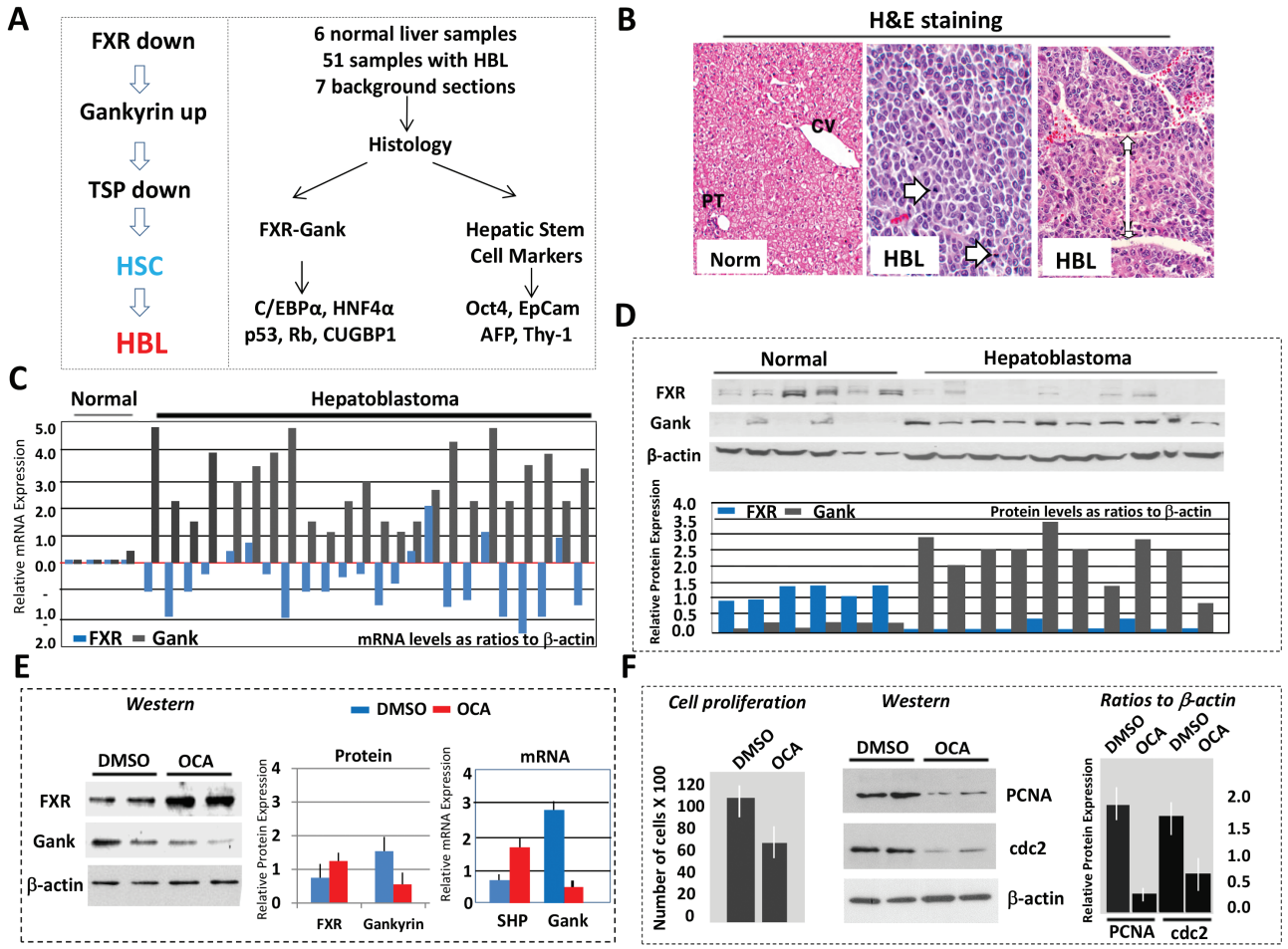

Figure 2. FXR is reduced and Gank is elevated in HBL samples. (**A**) Left: Proposed FXR-Gank-TSP pathway of HBL. Right: Liver cohort and approaches used for analysis of HBL samples. (**B**) H&E staining of normal liver and two HBL samples. Arrowheads show mitotic hepatocytes. Arrow shows macrotrabecular morphology with neoplastic cells arranged in plates of >5 cells thick. (**C**) Expression of FXR and Gank mRNAs in normal and HBL samples was examined by QRT-PCR and levels of mRNA levels are represented as ratios to β-actin. (**D**) Western blotting of nuclear extracts of normal and HBL samples with antibodies to FXR and Gank. (**E**) Left: Examination of protein and mRNA expression of FXR and Gank in HepG2 cells treated with 10uM OCA. Middle and right: bar graphs show levels of proteins and mRNAs correspondingly as ratios to β-actin. (**F**) OCA-dependent reduction of Gank inhibits proliferation of hepatoblastoma HepG2 cells. Left: Results of cell proliferation assay. Number of cells is shown at 48 hours after initiation of the OCA treatments. Western: Examination of cell cycle proteins PCNA and cdc2 by Western blotting. Right bar graphs show levels of PCNA and cdc2 as ratios to β-actin.

in HepG2 cells inhibits Gank resulting in the inhibition of cell proliferation.

Hepatocyte markers are reduced while stem cell markers are dramatically elevated in HBL samples

Since Gank supports high levels of stem cell marker Oct4 (25) and causes de-differentiation of hepatocytes into CSC (26), we suggested that the elevation of Gank in patients with HBL might block differentiation of HSC into hepatocytes. To test this hypothesis, we examined expression of markers of mature hepatocytes CYP3A4 and PEPCK, and markers of stem cells, Oct4, AFP, EpCam and Thy-1 in HBL samples. QRT-PCR analysis indicates that markers of hepatocytes are reduced in all HBL samples with different degrees of reduction (Figure 3A). We also found that markers of hepatocytes are reduced in all HBL samples on the level of proteins (Figure 3D). Examination of stem cell markers showed that all four markers are elevated in examined HBL samples. Importantly, we found that a significant group of HBL samples displayed a very high level of mRNA expression of the markers of Stem Cells which ranged from 50 to 5000 fold higher than in control livers (Figure 3B). Figure 3C and E show RT-PCR examination of hepatocyte markers and stem cell markers in additional HBL samples. Western blotting confirmed that markers of Stem Cells are also elevated on the levels of protein (Figure 3D). Interestingly, we also examined expression of albumin mRNA in HBL samples and found significant reduction of this mRNA in majority of HBL samples (Supplementary Figure 3). This reduction of the albumin mRNA in observed in all HBL patients with elevated levels of AFP. In a parallel study, we examined global transcriptome profiles of 31 HBL samples by RNA-Seq (Figure 4A). We detected alterations of multiple cancer-associated pathways such as activation of β-catenin, c-myc, TGFβ and WNT signaling and down-regulation of pathways involved in differentiation of HSC cells in hepatocytes. These global changes support the hypothesis that HBL is caused by a failure of HSC to differentiate in hepatocytes. These multiple alterations are under further investigations. In this paper, we focused on RNA-Seq results related to the FXR-Gank-TSPs axis. Alterations in FXR-Gank-HSC pathway are detected in all HBL samples using this approach (Figure 4B). RNA-Seq also identified alterations in additional mRNAs within both HSC markers and markers of hepatocytes (Figure 4B). Western blotting confirmed

these changes, displaying that CYP3A4 is dramatically reduced in all HBL samples, while PEPCK is reduced in a majority of HBL samples (see Figure 3D). RNA-Seq assays confirmed that expression of stem cell markers was significantly increased in HBL samples in comparison to normal tissue (Figure 4B). In addition, RNA-Seq assay revealed significant down-regulation of pathways of hepatocyte morphology and physiology (Figure 4A and B), which strongly support the hypothesis that differentiation of hepatocytes is inhibited in HBL.

Tumor suppressor proteins are reduced in a majority of HBL samples

During RNA-Seq analysis, we found that CUGBP1, p53 and Rb mRNAs were down-regulated in a majority of HBL samples. QRT-PCR confirmed these results. A typical picture of QRT-PCR results is shown in Figure 4C. Interestingly, C/EBPα and HNF4α mRNAs showed complex alterations with increased expression in some HBL samples. Figure 4C (bottom) shows results of QRT-PCR analysis of C/EBPα and HNF4α. In agreement with results of RNA-Seq and QRT-PCR, Western blotting showed that CUGBP1 and p53 are reduced in all examined HBL samples. C/EBPα and HNF4α are reduced in majority of HBL samples, however, a portion of HBL samples contained elevated levels of these proteins (Figure 4D).

Cyclin D1 expression showed that although protein levels are increased in a majority of HBL samples, mRNA levels are surprisingly reduced. Examination of fresh hepatoblastoma samples confirmed alterations of FXR-Gank-TSPs axis and elevation of stem cell markers (Supplemental Figure 4). Taken together, the studies of TSPs showed that the majority of HBL samples express reduced TSP mRNA and protein levels.

Livers of CUGBP1 KO mice have reduced markers of hepatocyte differentiation and have elevated markers of HSC

To understand if our findings in human HBL samples can be verified in, and translated to, animal models, we asked if the ablation of a TSP might inhibit differentiation of HSC into hepatocytes. For this goal, we chose CUGBP1 because it is reduced in a vast majority of HBL samples (Figure 4C). We have generated CUGBP1 KO mice and examined transcriptome profiles in livers of WT and CUGBP1 KO mice with the focus on regulation of markers of hepatocytes and markers of stem cells. Detailed characterization of the CUGBP1 KO mice is described in a separate manuscript (Wei et al., Manuscript Submitted). In this paper, we investigated liver biology of CUGBP1 KO mice. Since CUGBP1 KO mice die shortly after birth, we performed

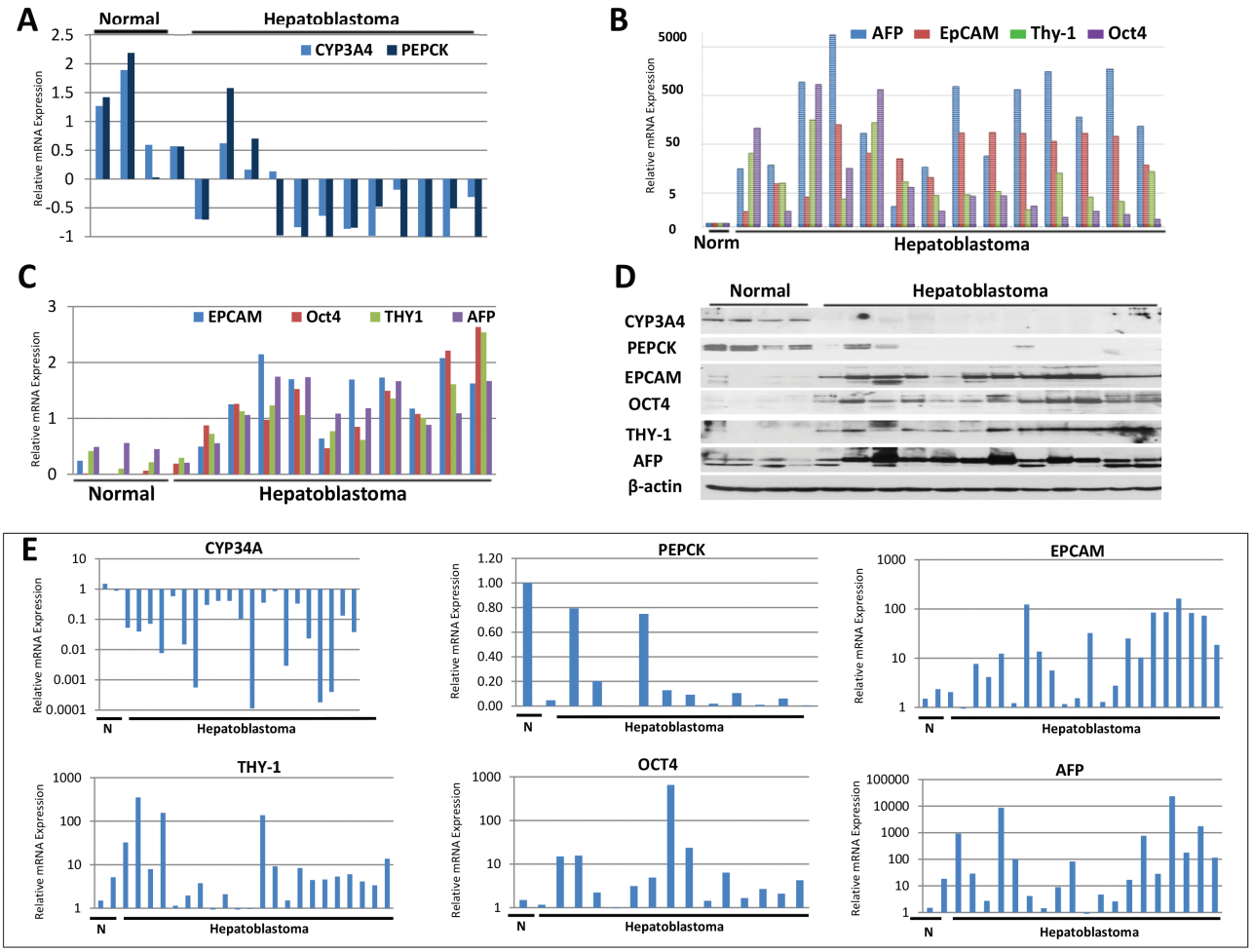

Figure 3. Hepatocyte markers are reduced, while stem cell markers are elevated in HBL samples (**A**) Levels of CYP3A4 and PEPCK mRNAs were determined by QRT-PCR. (**B** and **C**) Levels of mRNAs of stem cell markers were determined by QRT-PCR. (**D**) Examination of protein levels on markers of hepatocytes CYP3A4 and PEPCK and stem cells (EpCam, Oct4, Thy-1 and AFP) by Western blotting. Membrane was re-probed with Abs to β-actin. (**E**) Expression of mRNAs coding for CY3A4, PEPCK, AFP, EpCam, Oct4 and Thy-1 in additional samples of HBL.

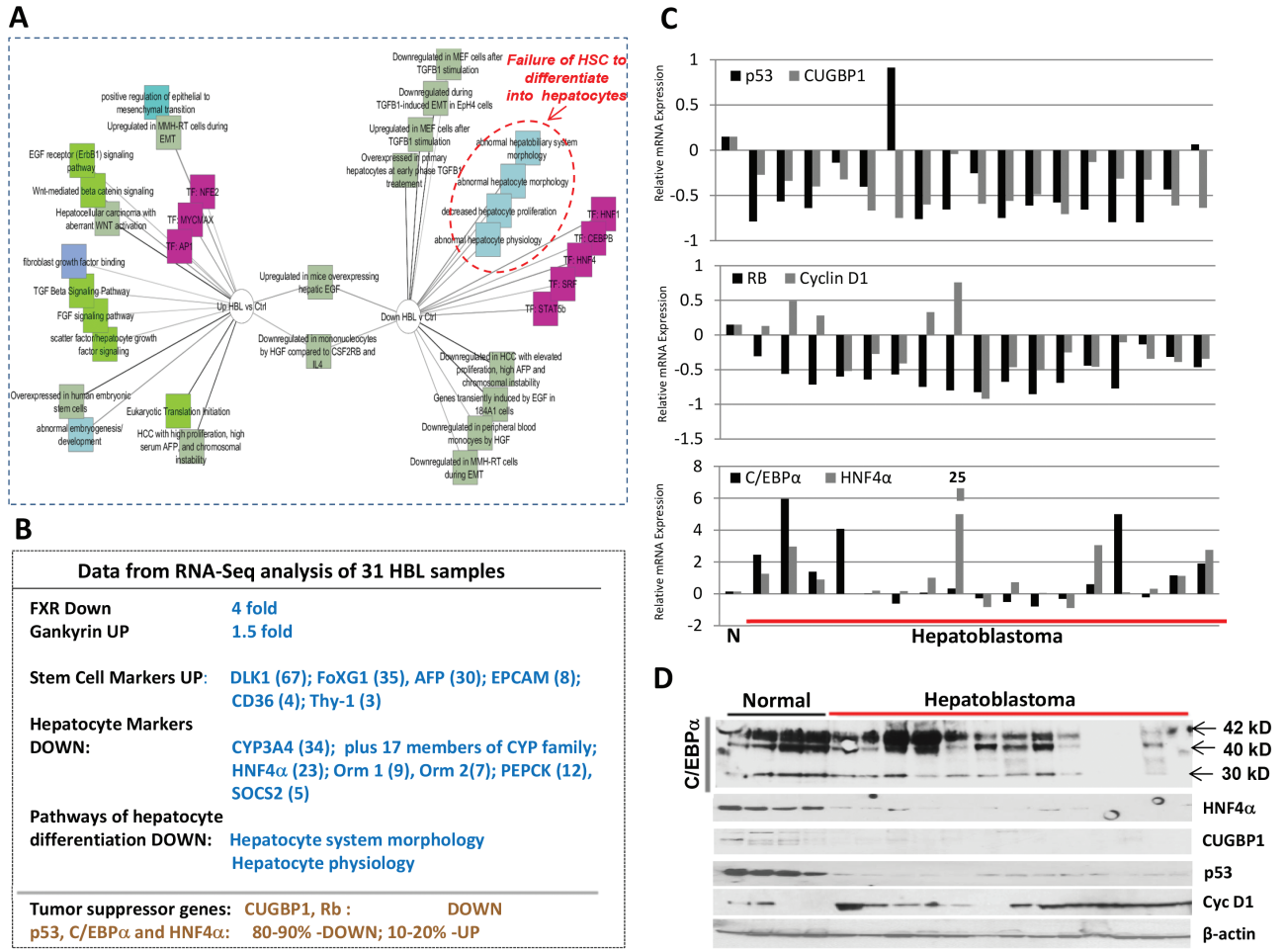

Figure 4. Molecular signature of hepatoblastoma: (**A**) RNA-Seq results displaying pathways up-regulated and down-regulated in analyzed HBL samples. Down-regulation of pathways of hepatocytes differentiation and physiology is shown by red circle. (**B**) Results of RNA-Seq analysis related to FXR-Gank-TSPs-Stem Cells axis. Fold change of mRNAs is shown in parenthesis. (**C**) Levels of mRNAs coding for p53, CUGBP1, C/EBPα and HNF4α were examined in normal (N) and hepatoblastoma cells by QRT-PCR and calculated as ratios to β–actin. (**D**) Western blotting of proteins from normal livers and HBL samples with antibodies to proteins shown on the right. 42kD, 40kD and 30kD isoforms of C/EBPα are shown. Membranes were re-probed with Abs to β-actin.

analysis of gene expression in 3-day-old mice. Western blotting and H&E staining of livers of CUGBP1 KO mice revealed that CUGBP1 is deleted with no significant changes in morphology at this stage of post-natal liver development (Figure 5A). However, micro-array analysis of these livers found dramatic alterations in gene expression (see heat map in Figure 5B). Figure 5C shows pathways that are altered in CUGBP1 KO mice livers. Alterations of these pathways include increases in expression of cell cycle genes and genes involved in cell proliferation. Importantly, nine markers of stem cells are up-regulated in livers of CUGBP1 KO mice and Orm family of markers of hepatocytes is down-regulated (Figure 5C and D). Interestingly, one CUGBP1-dependent stem cell markers, FoxG1, has been shown to be elevated in majority of HBL samples (27). It is also important to note that our RNA-Seq analysis also identified CUGBP1-dependent stem cell markers (Figure 5C and D) QRT-PCR confirmed that 5 markers of HSC are increased in livers of CUGBP1 KO mice (Figure 5D, bottom). Taken together, transcriptome profiling of livers of CUGBP1 KO mice strongly suggests that CUGBP1 is required for differentiation of hepatocytes perhaps by reprogramming stem cells into hepatocytes.

CUGBP1-dependent markers of HSC are elevated in HBL samples; while CUGBP1-dependent markers of mature hepatocytes are reduced

We next asked if the identified CUGBP1-dependent markers of HSC and hepatocytes are altered in human HBL. Initial studies with fresh and selected frozen HBL samples revealed that levels of FOXG1, MID1 and FOXP2 are increased in fresh and frozen HBL samples (Figure 6A); while ORM1, ORM2 and SOCS1 are reduced (Figure 6B). Elevation of CUGBP1-dependent markers of HSC and reduction of ORM family proteins were observed in all examined HBL samples (Figure 6C). Western blotting confirmed that SOCS1 is reduced and FOXG1 is increased in HBL samples (Figure 6D). Thus, these studies showed that CUGBP1-dependent markers of stem cells are elevated and CUGBP1-dependent markers of hepatocytes are reduced in examined HBL samples with reduced levels of CUGBP1. Taken together, we conclude that the FXR-Gank-TSP pathway is involved in regulating differentiation of HSC into hepatocytes and that alterations of this pathway contribute to the failure of HSC to differentiate into hepatocytes leading to the development of hepatoblastoma (Figure 6E).

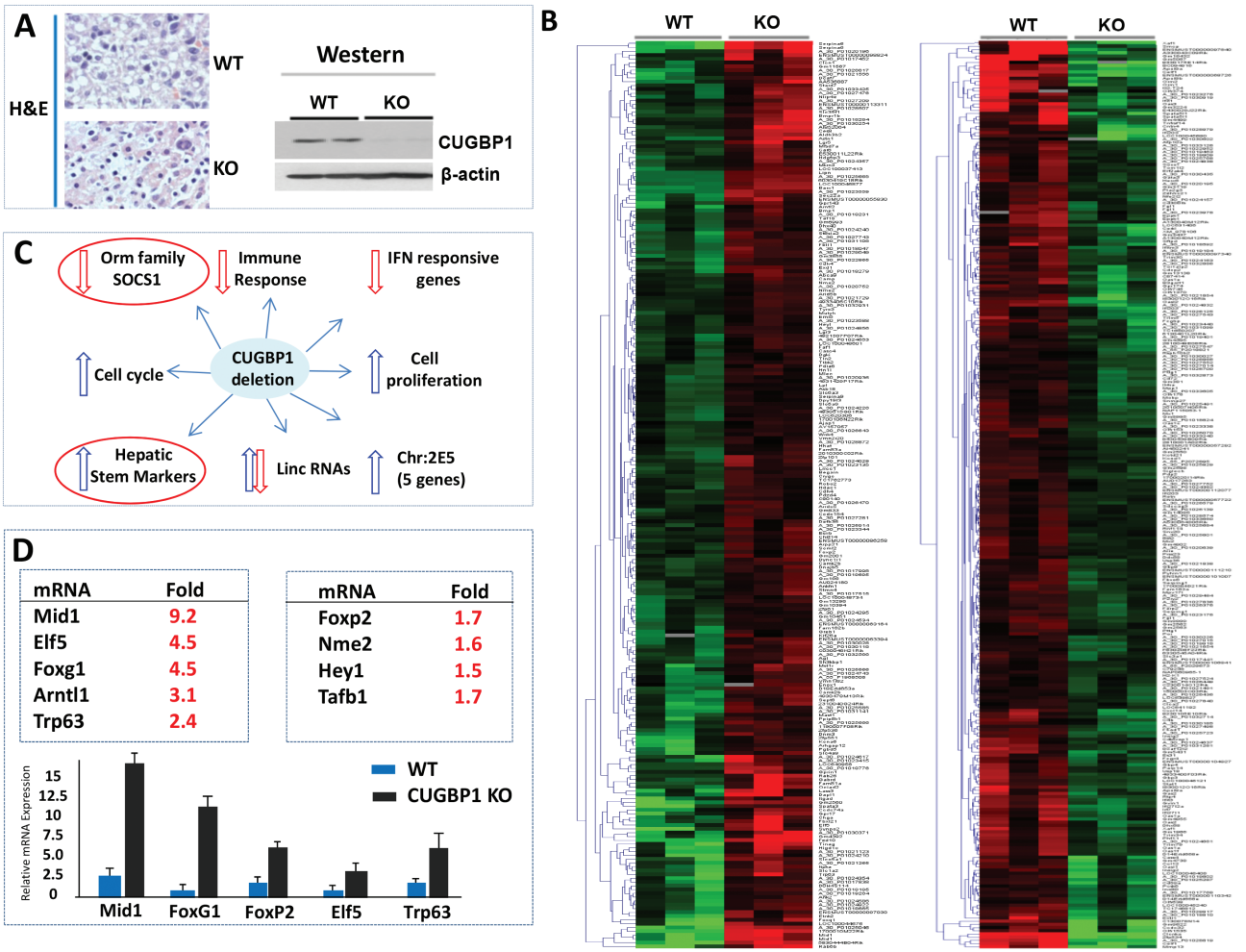

Figure 5. Livers of CUGBP1 KO mice show signatures of hepatoblastoma. (**A**) Left: H&E staining of livers of 3-day-old CUGBP1 KO and WT mice. Right: Western blotting analysis of CUGBP1 in livers of WT and CUGBP1 KO mice. (**B**) Micro-array-based heat map of genes which are elevated (left column) or down-regulated (right column) in livers of CUGBP1 KO mice. (**C**) Pathways with altered gene expression in livers of CUGBP1 KO mice determined by micro-array analysis. Pathways specific for stem cell markers (upper) and hepatocyte markers (lower) are circled in red. (**D**) Upper: Fold change in gene expression for markers of HSC in livers of CUGBP1 KO mice. Bottom: Expression of markers of HSC in livers of CUGBP1 KO mice by was determined QRT-PCR.

Discussion

Development of hepatocellular carcinoma in adults and the development of hepatoblastoma in children have different origins since HCC is frequently developed on the background of chronic liver diseases; while HBL occurs at very early stages of life. Our present work; however, demonstrates that they share significant similarities. Previous work in animal models of HCC found that the FXR-Gank axis plays a critical role in the development of HCC and that an elevation of Gank leads to elimination of tumor suppressor proteins (12,15). In this paper, we demonstrated that the activation of FXR inhibits the development of liver cancer in mice under the DEN protocol of carcinogenesis and that this inhibition involves the prevention of the activation of Gank and the subsequent rescue of tumor suppressor proteins. Our critical findings with this model in combination with previously published observations served as a strong rationale for our hypothesis which suggested that alteration of the FXR-Gank-HSC axis lead to the development of hepatoblastoma. In agreement with these data, Cairo *et al.* have found through global micro-array analysis that expression of Gank is increased in patients with HBL (18). Our observations in this current paper and those of several others suggest possible mechanisms by which increased Gank expression may cause HBL through activation of hepatic stem cells. These reports include findings that Gank supports tumor initiating cells by stabilization of OCT4 (24) and that Gank activates the WNT/β-catenin pathway which has been shown to be activated in HBL (18). It is important to mention that our findings in the newly generated CUGBP1 KO mice completely confirmed the main results of the studies of pediatric liver cancer. CUGBP1 protein is reduced in a majority of HBL samples and the global micro-array assay revealed that CUGBP1 KO mice display molecular signature of HBL; markers of hepatocytes are reduced, but markers of stem cells are elevated in HBL. Interestingly, all experiments carried out with HBL samples and livers of CUGBP1 KO mice are in good agreements with previous reports that showed the elevation of FOXG1 (27) and reduction of SOCS1 (28) in hepatoblastoma. Although our main hypothesis is that Gank blocks differentiation of HSC into hepatocytes, there is also a possibility that increased Gank expression might trigger HBL through de-differentiation of hepatocytes or other liver cells to cancer stem cells. In fact, Sun et al reported that Gank causes

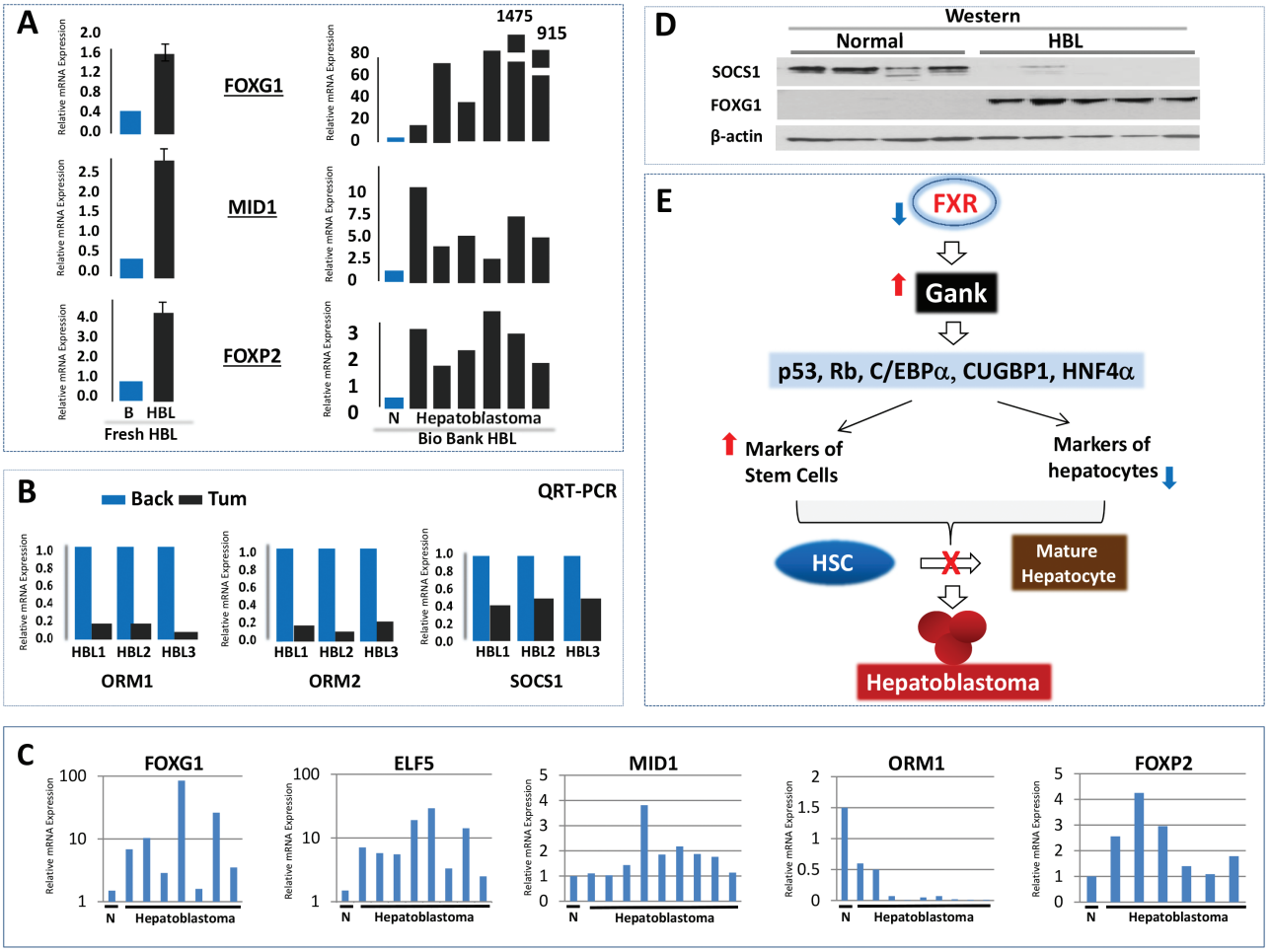

Figure 6. CUGBP1-dependent markers of hepatocytes are reduced; while CUGBP1-dependent markers of stem cells are elevated in pediatric liver cancer. (**A**) Expression of CUGBP1-dependent HSC markers in background, normal and HBL fresh and frozen liver tissues were determined by QRT-PCR. (**B**) CUGBP1-dependent markers of hepatocytes, ORM1, ORM1 and SOCS1 were examined in fresh HBL samples by QRT-PCR analysis. (**C**) CUGBP1-dependent markers of hepatocytes and stem cells were examined in additional frozen HBL samples. (**D**) Western blotting of CUGBP1-dependent SOCS1 and FOXG1 in control and HBL samples. (**E**) The proposed mechanism for development of HBL. This mechanism includes alterations of FXR-Gank-TSPs axis which lead to a block of differentiation of hepatic stem cells into hepatocytes.

de-differentiation of hepatocytes (26). Figure 6E summarizes our hepatoblastoma findings. We found that the majority of HBL samples have eliminated TSPs and a failure of hepatic stem cells to differentiate into hepatocytes. Although our results suggest mechanisms of pediatric liver cancer, we think that the FXR-Gank axis might also contribute to the development of liver cancer in adult patients by initiation of de-differentiation of hepatocytes in cancer initiating cells. This suggestion is in agreement with a report showing the reduction of FXR in adult patients with HCC (29). Therefore, we believe that our findings may be further used for the development of FXR-Gank based and TSPs-based approaches for the prevention and treatments of pediatric liver cancer and liver cancer in adult patients. In this regards, it is important to mention two recent reports which showed that the activation of the tumor suppressor protein C/EBPα by short activating RNA (saRNA) inhibits HCC in rat models of liver cancer (30) and in nude mice transfected with HepG2 cells expression saRNA to C/EBPα (31). These two studies also demonstrated that the rescue of C/EBPα expression in cultured cells and in nude mice resulted in significant improvements of liver functions. Interestingly, activation of C/EBPα by saRNA in HepG2 cells also resulted in an increase in expression of 18 additional TSPs (30).

One of the key findings of our paper is the identification of the activation of the FXR-Gank axis as a critical incident which operates up-stream of tumor suppressor proteins and causes the failure of HSC to differentiate into hepatocytes. At this stage, very little is known regarding therapeutic options that can reduce or eliminate Gank activities. A recent paper has described the discovery of a small molecule termed cjoc42 which binds to Gank and prevents degradation of p53 (32). While Gank-mediated therapy is limited, there is more promising evidence towards FXR as a possible target to treat HCC and HBL. As one can see in Figure 2, obeticholic acid (OCA) significantly reduces expression of Gank by activating FXR leading to inhibition of cell proliferation. It is important that activation of FXR by OCA is in several trials with NAFLD patients for both trials Phase II and Phase III (33). Our data suggest that OCA is a potential drug which could be fast used in clinical trials with liver cancer patients. In summary, our work shows key molecular mechanisms of HBL and provides a molecular basis for possible therapeutic treatments targeting members of the FXR-Gank-TSPs axis.

Supplementary Material

Supplementary data are available at *Carcinogenesis* online.

Funding

This work is supported by NIH R01CA159942 and R01DK102597 (N.T.); by Internal Development Funds from CCHMC (N.T. and L.T.), by NIH grants AR052791, AR064488 (L.T.) and by P30 DK078392 (D.W.).

Acknowledgements

We thank Dr. M.Finegold and Dr. D.Moore for the discussion of the results with GW4064-mediated activation of FXR. We thank Christina Wei for help with CUGBP1 KO mice.
Conflict of Interest Statement: None declared.

References

1. Oishi, N. et al. (2014) Molecular biology of liver cancer stem cells. Liver Cancer, 3, 71–84.
2. Carter, A.J.R. et al. (2012) A comparison of cancer burden and research spending reveals discrepancies in the distribution of research funding. BMC Public Health., 12, 26–38.
3. Martin, J. et al. (2008) Tumor suppressor and hepatocellular carcinoma. World J. Gastroenterol., 14, 1720–1733.
4. Callegari, E. et al. (2015) MicroRNAs in liver cancer: a model for investigating pathogenesis and novel therapeutic approaches. Cell Death Differ., 22, 46–57.
5. Yin, H. et al. (2014) MicroRNAs as a novel class of diagnostic biomarkers in detection of hepatocellular carcinoma: a meta-analysis. Tumour Biol., 35, 12317–12326.
6. Khare, S. et al. (2013) Epigenetics of hepatocellular carcinoma: role of microRNA. World J. Gastroenterol., 19, 5439–5445.
7. Revill, K. et al. (2013) Genome-wide methylation analysis and epigenetic unmasking identify tumor suppressor genes in hepatocellular carcinoma. Gastroenterology, 145, 1424–35.e1.
8. Xue, W. et al. (2012) A cluster of cooperating tumor-suppressor gene candidates in chromosomal deletions. Proc. Natl. Acad. Sci. USA, 109, 8212–8217.
9. Aguirre, E. et al. (2014) Genetic Modeling of PIM Proteins in Cancer: Proviral Tagging and Cooperation with Oncogenes, Tumor Suppressor Genes, and Carcinogens. Front. Oncol., 4, 109.
10. Dawson, S.P. (2008) Hepatocellular carcinoma and the ubiquitin-proteasome system. Biochim. Biophys. Acta, 1782, 775–784.
11. Iakova, P. et al. (2011) Intracellular signaling and hepatocellular carcinoma. Semin. Cancer Biol., 21, 28–34.
12. Timchenko, N.A. and Lewis, K. (2015) Elimination of tumor suppressor proteins during liver carcinogenesis. Cancer Stud. Mol. Med., 1, 27–38.
13. Lim, I.K. (2003) Spectrum of molecular changes during hepatocarcinogenesis induced by DEN and other chemicals in Fisher 344 male rats [Mechanisms of Ageing and Development 123 (2002) 1665-1680]. Mech. Ageing Dev., 124, 697–708.
14. Wang, G.L. et al. (2010) Elimination of C/EBPalpha through the ubiquitin-proteasome system promotes the development of liver cancer in mice. J. Clin. Invest., 120, 2549–2562.
15. Jiang, Y. et al. (2013) Farnesoid X receptor inhibits gankyrin in mouse livers and prevents development of liver cancer. Hepatology, 57, 1098–1106.
16. Luo, J.H. et al. (2006) Transcriptomic and genomic analysis of human hepatocellular carcinomas and hepatoblastomas. Hepatology, 44, 1012–1024.
17. Cairo, S. et al. (2008) Hepatic stem-like phenotype and interplay of Wnt/beta-catenin and Myc signaling in aggressive childhood liver cancer. Cancer Cell, 14, 471–484.
18. Cairo, S. et al. (2010) Stem cell-like micro-RNA signature driven by Myc in aggressive liver cancer. Proc. Natl. Acad. Sci. USA, 107, 20471–20476.
19. Eichenmüller, M. et al. (2014) The genomic landscape of hepatoblastoma and their progenies with HCC-like features. J. Hepatol., 61, 1312–1320.
20. Wolfe, A. et al. (2011) Increased activation of the Wnt/β-catenin pathway in spontaneous hepatocellular carcinoma observed in farnesoid X receptor knockout mice. J. Pharmacol. Exp. Ther., 338, 12–21.
21. Guo, Z. et al. (2014) Cancer stem cell markers correlate with early recurrence and survival in hepatocellular carcinoma. World J. Gastroenterol., 20, 2098–2106.
22. Timchenko, L.T. et al. (1996) Identification of a (CUG)n triplet repeat RNA-binding protein and its expression in myotonic dystrophy. Nucleic. Acids Res., 24, 4407–4414.
23. Jones, K. et al. (2012) The role of CUGBP1 in age-dependent changes of liver functions. Ageing Res. Rev., 11, 442–449.
24. Ali, H. et al. (2015) Recent advances in the development of farnesoid x receptor agonists. Ann. Transl. Med., 3, 5.
25. Qian, Y.W. et al. (2012) p28(GANK) prevents degradation of Oct4 and promotes expansion of tumor-initiating cells in hepatocarcinogenesis. Gastroenterology, 142, 1547–58.e14.
26. Sun, W. et al. (2011) Gankyrin-mediated dedifferentiation facilitates the tumorigenicity of rat hepatocytes and hepatoma cells. Hepatology, 54, 1259–1272.
27. Adesina, A.M. et al. (2007) FOXG1 is overexpressed in hepatoblastoma. Hum. Pathol., 38, 400–409.
28. Chu, P.Y. et al. (2010) Epigenetic alteration of the SOCS1 gene in hepatocellular carcinoma. Swiss Med. Wkly., 140, w13065.
29. Wolfe, A. et al. (2011) Increased activation of the Wnt/β-catenin pathway in spontaneous hepatocellular carcinoma observed in farnesoid X receptor knockout mice. J. Pharmacol. Exp. Ther., 338, 12–21.
30. Reebye, V. et al. (2014) Novel RNA oligonucleotide improves liver function and inhibits liver carcinogenesis in vivo. Hepatology, 59, 216–227.
31. Huan, H. et al. (2016) C/EBPα Short-Activating RNA Suppresses Metastasis of Hepatocellular Carcinoma through Inhibiting EGFR/β-Catenin Signaling Mediated EMT. PLoS One, 11, e0153117.
32. Chattopadhyay, A. et al. (2016) Discovery of a small-molecule binder of the oncoprotein gankyrin that modulates gankyrin activity in the cell. Sci. Rep., 6, 23732.
33. Neuschwander-Tetri, B.A. et al.; NASH Clinical Research Network. (2015) Farnesoid X nuclear receptor ligand obeticholic acid for non-cirrhotic, non-alcoholic steatohepatitis (FLINT): a multicentre, randomised, placebo-controlled trial. Lancet, 385, 956–965.